Marine Geology 470 (2024) 107267

Contents lists available at ScienceDirect

Marine Geology

journal homepage: www.elsevier.com/locate/margo

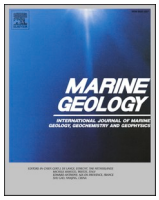

Research Article

Computed Laminography for the study of biogenic structures in sediment cores: A step between two- and three-dimensional imaging

Javier Dorador [a,*], Francisco J. Rodríguez-Tovar [a], Miros S.J. Charidemou [b], Olmo Miguez-Salas [a,c]

[a] Department of Stratigraphy and Palaeontology, Universidad de Granada, Granada, Spain
[b] British Ocean Sediment Core Research Facility, National Oceanography Centre, European Way, Southampton SO14 3ZH, United Kingdom
[c] Department of Marine Zoology, Senckenberg Research Institute and Natural History Museum, Frankfurt, Germany

ARTICLE INFO

Editor: Shu Gao

Keywords:
Image treatment
Non-invasive techniques
Internal structures
Deep-sea settings
Bioturbation

ABSTRACT

The study of trace fossils —ecological indicators of environmental parameters such as organic-matter content, oxygenation or sedimentation rate, among others— is a powerful tool for analysing cores from deep-sea sediment. However, the visualization of biogenic structures in soft sediment cores is commonly poor. This problem has usually been solved by using X-ray radiographs from core slabs, and later by non-destructive Computed Tomography (CT). Yet the latter requires complex processing and computer resources to deal with a vast dataset. Computed Laminography (CL) stands as an alternative, non-destructive technique able to manage a small amount of data, providing results similar to X-ray radiographs. This technique is frequently used in other disciplines (e.g. material sciences), but rarely applied in geosciences. In the present study, we explore the usefulness of CL for studying the ichnological content of modern deep-sea deposits from boxcores collected from the Porcupine Abyssal Plain (NE Atlantic). Additionally, we compare results from Linear CL (LCL) and Circumferential CL (CCL) to discuss which is recommended depending on the goal involved. The obtained results confirm the usefulness of CL for the ichnological analysis of sediment cores, with similar results from LCL and CCL. However, recommendations are made to resolve doubtful scenarios and to save time. In light of our findings, the use of CL as a non-destructive technique, calling for a much smaller dataset than CT, can be highly recommended for the study of ichnological content or other internal structures.

1. Introduction

Ichnological analysis of core samples is a well-established method used to characterise and interpret the subsurface, but it typically allows observations to be made only on a narrow exposure of a split or slab core, and only bidimensional features are identified (Gérard and Bromley, 2008; Knaust, 2012, 2017; Dorador and Rodríguez-Tovar, 2018). Several techniques may be applied to gather information beyond what is visible on the exposed core surface. For example, when working with sediment cores — especially from deep-sea deposits — X-ray techniques serve to characterise internal structures (e.g., Löwemark, 2007). Radiographs have been successfully applied for analysing internal features such as sedimentary structures (e.g., Andrews et al., 1997; Dowdeswell et al., 2000) and bioturbation (e.g., Aller and Aller, 1986; Wetzel, 2010; Dashtgard et al., 2015) from cores and box-cores. Historically, X-radiographs from sediment cores were obtained by scanning 1- to 2-cm thick slabs of the original core, which was not only a destructive technique, but often caused disturbance to the sedimentary features under study (e.g., Dashtgard et al., 2015). Over the last few decades, X-radiography has been largely replaced by non-destructive Computed Tomography (CT) techniques (e.g., Cnudde and Boone, 2013). CT has proven to be a powerful tool for the study of sediment cores when focusing on sedimentology, stratigraphy, permeability, fracturing or ichnology (e.g., Orsi et al., 1994; Boespflug et al., 1995; Ellis et al., 2013; Konno et al., 2016; Wang et al., 2019; Dorador et al., 2020).

The application of CT for ichnological studies is particularly useful in characterising and quantifying the three-dimensional morphology, connectivity, and volume of burrows (e.g., Dorador and Rodríguez-Tovar, 2020; Dorador et al., 2020; Dorador et al., 2020; Eltom et al., 2023). Still, the application of CT techniques in the framework of sediment cores, and ichnology in particular, also presents certain challenges.

* Corresponding author.
E-mail address: javidr@ugr.es (J. Dorador).

https://doi.org/10.1016/j.margeo.2024.107267
Received 2 January 2024; Received in revised form 1 March 2024; Accepted 10 March 2024
Available online 12 March 2024

The relatively large dimensions of sediment cores (50 to 150 cm length and 5 to 15 cm diameter) preclude them from being scanned in Micro-CT scanners, which are able to provide images with very high resolution. Sediment cores are commonly scanned in medical scanners, or specialist core scanners, whose resolution may be too low to resolve the sub-millimetric structures of certain trace fossils. Additionally, some internal structures of interest for ichnological studies may remain undetectable using standard CT processing methods, as the density contrast between the trace fossil fill and the host material is very low. This drawback is particularly apparent in unconsolidated sediments. Finally, the large volumes of data generated from CT scans of sediment cores, plus the large file sizes of reconstructed volumes, requires powerful workstations that may not be readily accessible for processing, analysing and visualizing the data.

Computed Laminography (CL) is an alternative to older radiography and CT techniques. CL is a non-destructive X-ray method that can produce cross-sectional images of samples, similar to CT. The main difference is that in CT the X-ray beam rotates perpendicular to the object, whereas in CL the beam is inclined, reaching angles that are inaccessible to CT scanning (Xu et al., 2012; Gondrom et al., 1999, O'Brien et al., 2016). In CL the sample is horizontally translated through the X-ray cone-beam to irradiate the object under different angles within the beam. This produces a stack of cross-sectional images from different depths within the sample, making it is possible to characterise internal structures in three-dimensional space (e.g., Moore et al., 2002). Importantly, CL can be applied using a conventional CT scanner (Fisher et al., 2019) and affords better spatial resolution than medical CT scanners (Zuber et al., 2017; McDonald et al., 2022). It is very well suited for planar and small flat objects studied under synchrotron radiation, where CT is less successful (e.g., Bull et al., 2013), in material sciences (e.g., Helfen, 2005; Morgeneyer et al., 2011; Verboven et al., 2015), microsystem inspection (e.g., Helfen, 2005) and art studies (e.g., Legrand et al., 2014), among others. To date, however, this technique has scarcely been explored in the earth sciences. The handful of studies published includes just a few palaeontological studies on planar fossils (e.g., Houssaye et al., 2011; Zuber et al., 2017) and a recent study on sediment cores to characterise glaciomarine sediments (McDonald et al., 2022). Here, we use CL for the first time to study biogenic structures, specifically of 49 sediment cores extracted from two box-cores from the Porcupine Abyssal Plain (c. 4850 m depth), Northeast Atlantic. The main aim of our study is to determine whether this non-destructive technique can be successfully applied for bioturbation analysis. Especially relevant is the fact that in some cases CT cannot deal with the computational challenges of working with large volumes of data, restrictive costs, and/or limitations related to the maximum obtainable resolution of CT scans of sediment cores. We verify that bioturbation structures can be visualized under this technique, and we analyse the ichnological content by focusing on the identification of trace fossils and the quantification of the bioturbated surface, comparing the results from different slices in each core. In addition, we compare Linear and Circumferential Computed Laminography (LCL and CCL) data to test which is the best acquisition method for studying internal structures in sediment cores.

2. Methodology

Box-cores were obtained from two locations within the Porcupine Abyssal Plain Sustained Observatory area (PAP-SO) during RRS James Cook cruise 231 (Hartman, 2022) (Fig. 1). They include: 1) the flank of a single small abyssal hill (JR231_BC049, extracted May 8th, 2022); H3 sensu Durden et al., 2015; and 2) an open abyssal plain location (JR231_BC019, collected May 5th, 2022); referred as 'PAP central' in Durden et al. (2020). From each box-core, twenty-five 8 cm diameter cores were extracted with 65 cm long core liners (Fig. 1B), right after dewatering. One of the cores was discarded owing to preservation issues, so that finally 49 sediment cores were analysed. These cores were stored at low temperature (i.e., 6° Celsius), keeping a natural and stable

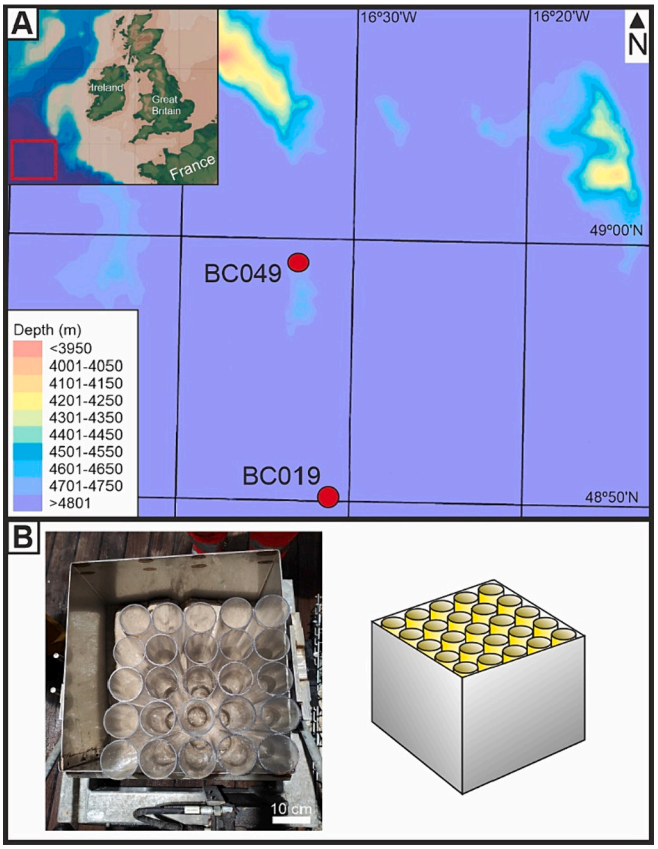

Fig. 1. Boxcore location and sampling. A, location of studied boxcores at the Porcupine Abyssal Plain; B, picture and diagram of core liner in one of the boxcores.

orientation to avoid sediment mixing.

All the cores were scanned during the next months (from June to August 2022) at the British Ocean Sediment Core Research Facility (BOSCORF) in Southampton (UK) using a Geotek ScoutXcan multi-angle digital 2D X-ray System. On this system, core samples are loaded horizontally and secured between two motorised arms within a shielded cabinet. The core sample is then translated horizontally between an X-ray source and flat panel detector. The motorised arms are also able to rotate around their axes, making it possible to acquire multiple 2D radiographs at various orientations throughout the sample.

The core samples are set up for scanning using an experimental optimisation approach. The workflow involves adjusting the source-to-sample distance and the source-to-detector distance, evaluating the resulting image quality to find the best compromise between magnification, resolution, and field of view. In the current study the sample was located 23.5 cm from the X-ray source and 40 cm from the detector (Fig. 2A).

The Geotek ScoutXcan uses a 65 W Thermo Kevex 130 kV Microfocus X-ray source with a tungsten target and a Varex Imaging 1920 × 1536 pixel flat panel detector. The X-ray tube was set with a voltage of 115 kV and a current of 425 μA. The X-ray beam was passed through a 1.0 mm Cu filter. The resultant beam spot size was 73 μm and the image resolution was 212.9 pixels cm^{-1} (i.e., 540.77 dpi).

LCL and CCL images were reconstructed from the raw radiographic projection data acquired for each core sample using the Geotek Reconstructor proprietary software. The reconstructed LCL images represent horizontal slices from different depths through the core sample. For the current study, seven slices from each core were reconstructed at +30 mm, +20 mm, +10 mm, 0 mm, − 10 mm, −20 mm, and − 30 mm (0 mm being the slice crossing the central axis of the core; Fig. 2B). The

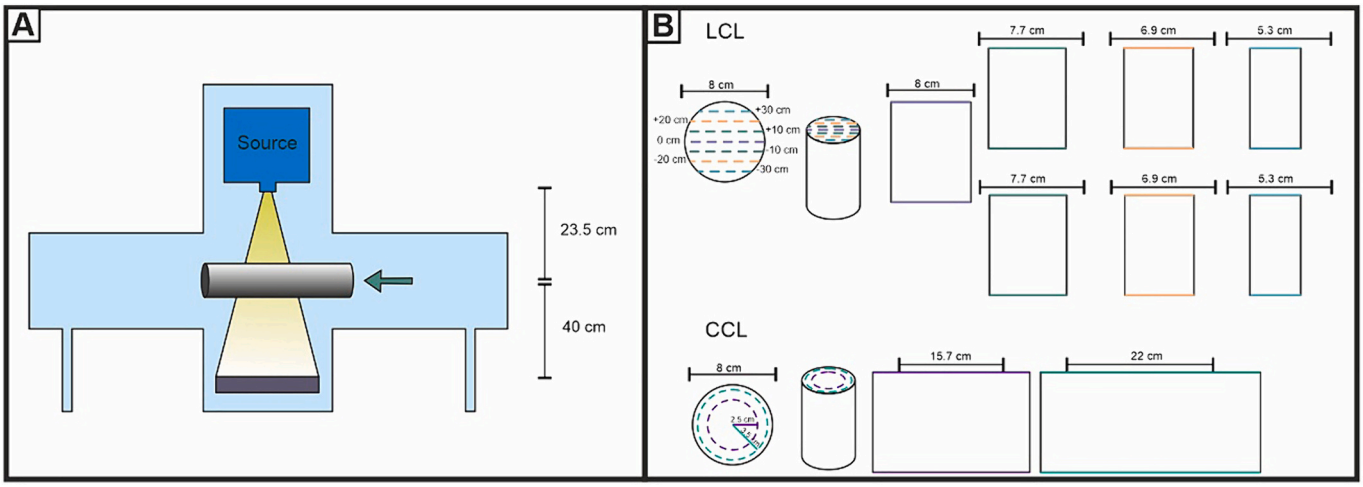

Fig. 2. Computed Laminography (CL) acquisition. A, Scheme of CL scanning; and B, outputs from Linear CL (LCL) and Circumferential CL (CCL).

reconstructed CCL images represent unwrapped cylindrical views from different radii along the central axis of each core. In the study presented here, two CCL images were reconstructed from every core at 25 mm and 35 mm radii (Fig. 2B). In total, 441 images were generated for the 49 cores analysed.

All the images were treated to improve trace-fossil visualization as they were not clearly distinguishable in the original images (Fig. 3). The image treatment was mainly based on the sequence developed by Dorador et al. (2016) for deep-sea sediment cores, which has been usefully applied in previous studies (e.g., Rodríguez-Tovar et al., 2015; Alonso et al., 2016; Dorador and Rodríguez-Tovar, 2016; Dorador et al., 2016; Hodell et al., 2017; Gougeon et al., 2018; González-Lanchas et al., 2022; Valencia et al., 2022). This procedure entails three image adjustments: (1) levels, (2) brightness/contrast, and (3) intensity, which are normally modified to enhance the visualization of trace fossils. However, in the present study intensity was not applied; it was replaced by an exposition adjustment conducted by a gamma correction tool, providing for better results in this particular case (Fig. 3).

The intensity of bioturbation was characterised by calculating the bioturbated surface in each image of ten selected cores, five from each box-core. Then, nine values were obtained from every analysed core

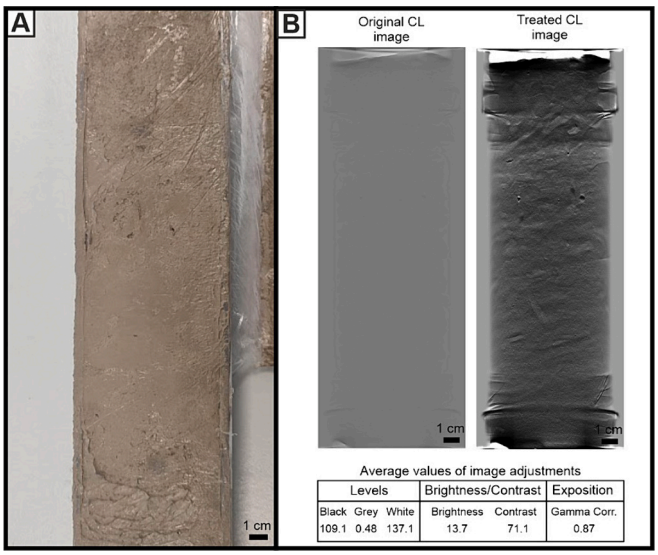

Fig. 3. Image treatment. A, example of a gravity core extracted from the same area; and B, example of Computed Laminography (CL) image treatment from one of the cores, and average values after processing all the images.

—seven from LCL images and two from CCL. Additionally, shorter intervals were considered in every image, differentiating top, middle and bottom core intervals; shorter intervals are usually considered in ichnological analysis to characterise shallow, middle, and deep traces. Comparisons between sections and shorter intervals, considering both types of CL images, served to assess which would be the most appropriate acquisition method for estimating the intensity of bioturbation. The percentage of bioturbated surface was used to determine the Bioturbation Index (BI). This is a commonly used scale, divided in seven degrees from 0 (no bioturbation) to 6 (fully bioturbated), proposed by Reineck (1963) and later revised by Taylor and Goldring (1993). In the present study, the analysed intervals fall within BI 1 (1–4%) and BI 2 (5–30%).

3. Results

3.1. Characterization of trace fossils

Trace-fossil identification was no easy matter because cores were taken directly from the seafloor, recording the uppermost unconsolidated sediments, which are topped by the soupy mixed layer (a water-saturated and fully bioturbated interval in the uppermost centimetres) (Teal et al., 2008). Thus, every primary sedimentary structure is reworked and, due to sediment aggradation, the record of the mixed layer is recognized in the background of the whole core as a mottling texture (Bromley, 1996). Regardless, thirteen discrete biogenic structures, overlapping the mottled background, were identified in the images. Identification reached the ichnogenus level in those cases where ichnotaxobases (i.e., characteristic morphological features; Bromley, 1996; Bertling et al., 2022) were observed, but ichnospecies were not defined in any case.

Specifically, we were able to differentiate some radiating burrows as *Asterosoma* and *Parahaentzschelinia* (Fig. 4A), small branching tunnel systems as *Chondrites*, and some larger and passively filled galleries interpreted as *Thalassinoides* (Fig. 4B). Small, horizontal patches were associated with patterned trace fossils grouped as graphoglyptids, and other structures commonly produced in the uppermost centimetres on deep-sea settings as potential *Helicodromites* and *Nereites* (Fig. 4C). Subhorizontal cylindrical tubes associated with *Palaeophycus* and *Planolites* (Fig. 4D), and some curved subvertical tubes interpreted as *Schaubcylindrichnus* (Fig. 4E), were also recognized. Horizontal bi- or trilobed backfilled burrows were associated with *Scolicia* (Fig. 4F), and subhorizontal spreite structures crossing the entire core were tentatively ascribed to *Zoophycos* (Fig. 4G). Some tiny filaments commonly associated with "mycelia" (Fig. 4H) were identified. Real examples of the

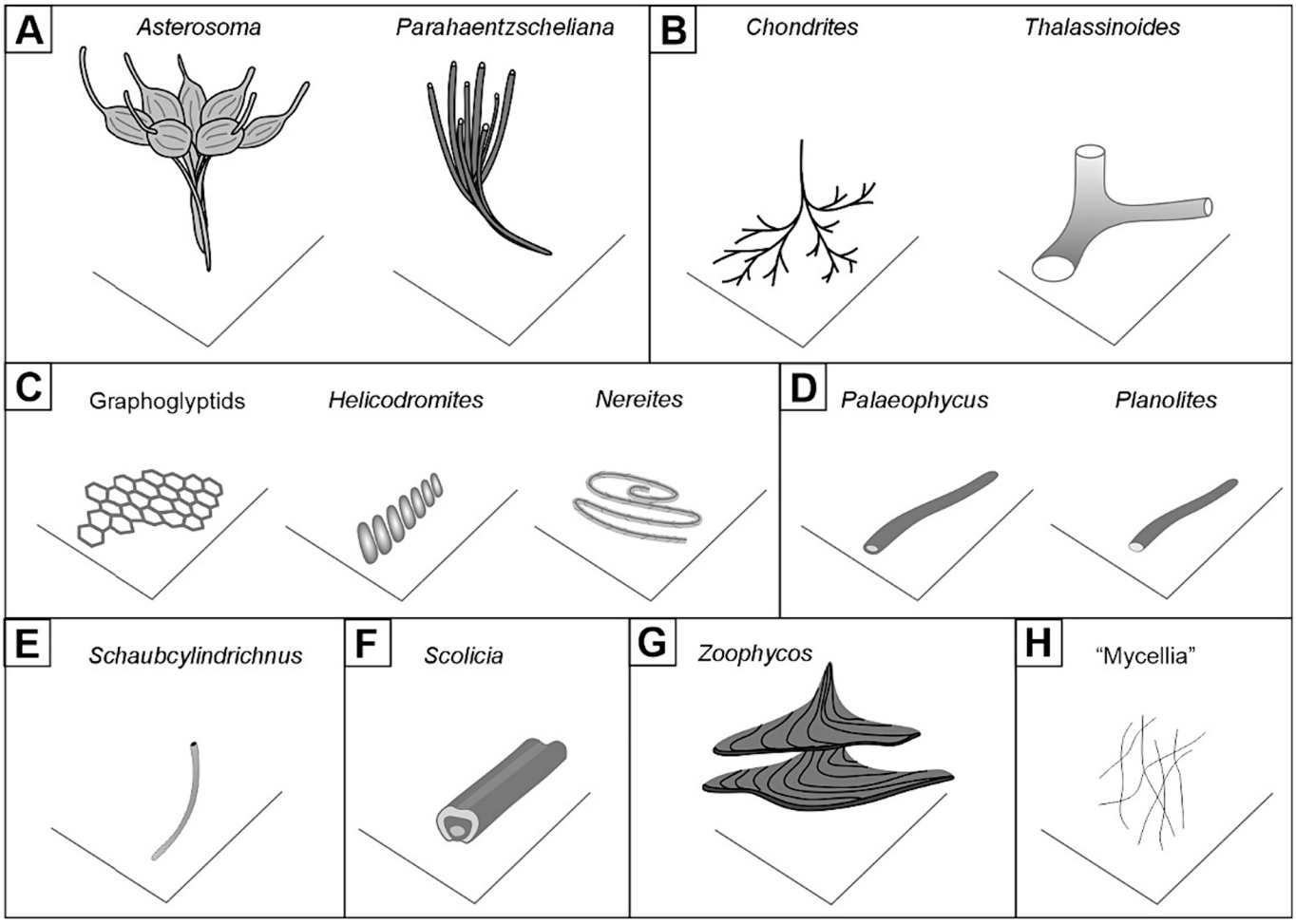

Fig. 4. Schematic diagrams of characterised trace fossils grouped based on their morphological features.

identified trace fossils from LCL and CCL images can be observed in Fig. 5.

3.2. Intensity of bioturbation

To characterise the intensity of bioturbation, the surface occupied by trace fossils was quantified in every slide, considering the entire section, but also at shorter areas (top, middle, and bottom intervals). Here we illustrate a representative example from the ten analysed cores: sediment core sample 15 from box-core 49 (Fig. 6, Table 1). It should be noted that the values obtained from CCL images are underestimated due to limited visibility in some vertical regions of the images. These blurred

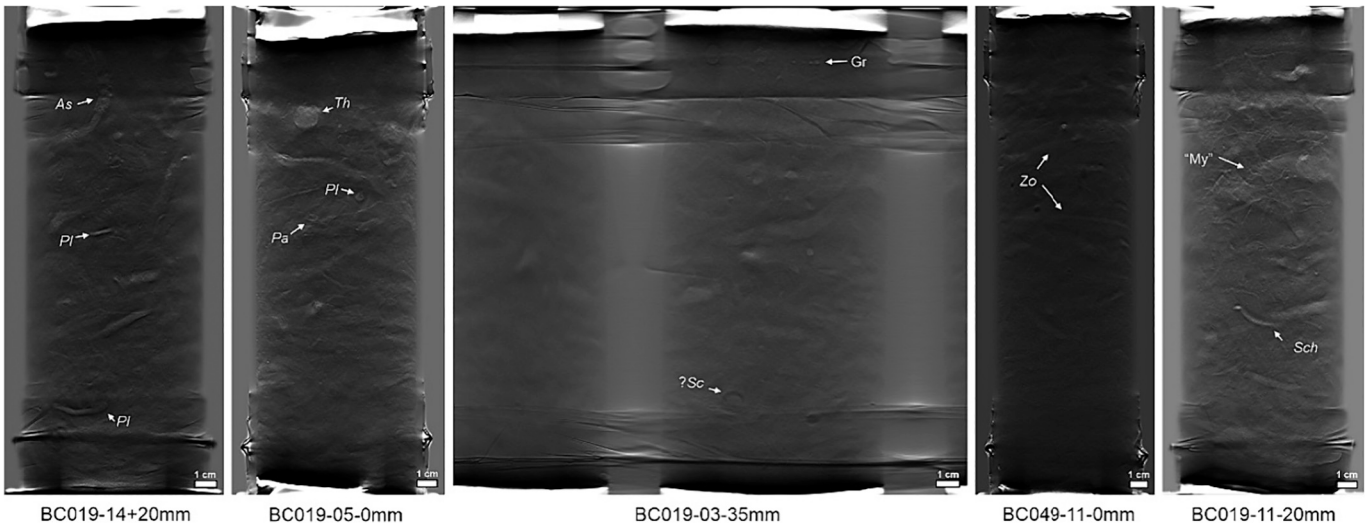

Fig. 5. Examples of trace fossils identified in LCL and CCL images from the study cores.

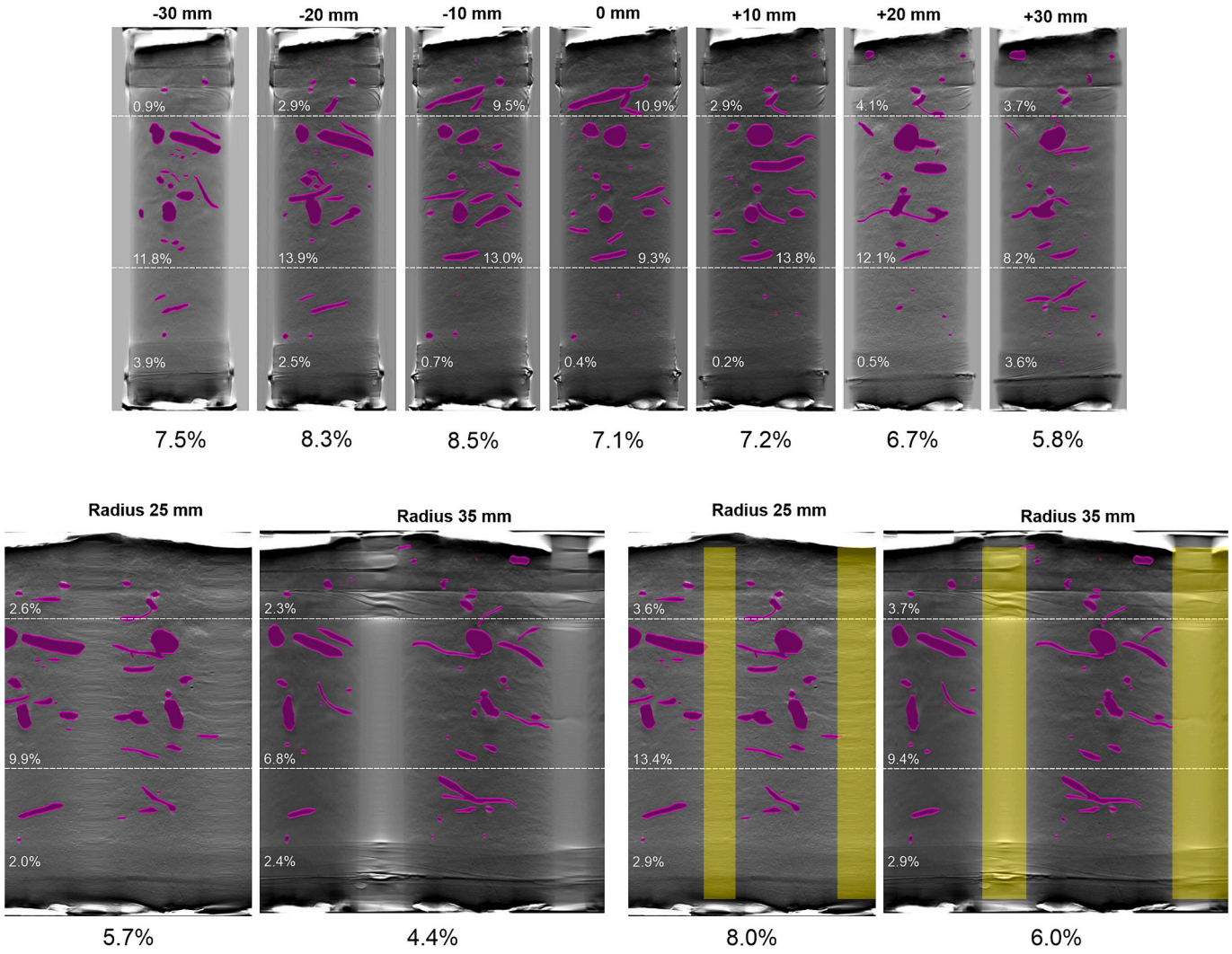

Fig. 6. Quantification of bioturbated surface in images from LCL (above) and CCL (below) images from one of the cores. In the bottom right corner images, values are recalculated removing the shadow areas (yellow in colour version). Black numbers refer to the whole core section and numbers in white are from shorter intervals. (For interpretation of the references to colour in this figure legend, the reader is referred to the web version of this article.)

Table 1
Quantification of bioturbation. Percentages of bioturbated surface in every interval. LCL, Linear Computed Laminography; CCL, Circumferential Computed Laminography.

	LCL							CCL		Mean LCL	Mean CCL	Mean	Stand. Dev.
	−30 mm	−20 mm	−10 mm	0 mm	10 mm	20 mm	30 mm	Radius 25 mm	Radius 35 mm				
Top Interval	0.9	2.9	9.5	10.9	2.9	4.1	3.7	3.6	3.7	5.0	3.7	4.7	3.3
Middle Interval	11.8	13.9	13.0	9.3	13.8	12.1	8.2	13.4	9.4	11.7	11.4	11.7	2.2
Bottom Interval	3.9	2.5	0.7	0.4	0.2	0.5	3.6	2.9	2.9	1.7	2.9	2.0	1.5
Whole section	7.5	8.3	8.5	7.1	7.2	6.7	5.8	8.0	6.0	7.3	7.0	7.2	1.0

areas occur because the X-ray beams cross the sample at angles close to the tangent of the reconstructed circumference through the core. Such artefacts are easily corrected to ensure that bioturbation quantifications avoid these regions (yellowish in Fig. 6).

Regarding values obtained from the whole sections, in Linear Computed Laminography (LCL) images, the bioturbated surface ranges from 5.8% to 8.5%, having a mean value of 7.3% (Fig. 6, Table 1). All of them represent Bioturbation Index (BI) 2 that ranges from 6% to 30% of bioturbation. Similar values are obtained from Circumferential Computed Laminography (CCL), for which the average is 7%.

Regarding shorter intervals within the sections, differences are higher in some cases, being especially notable for top intervals. For LCL images, the top interval values range from 0.9% to 10.9%, with a mean value of 5.0% pertaining to BI 2. In turn, the average from CCL is 3.7%, which corresponds to BI 1 (1–4%). Moreover, its BI classification would be different (i.e., BI 2) in some cases if the bioturbated surface were calculated just from a single image (e.g., 0 mm LCL) instead of using the mean value of all images. In the middle intervals, bioturbated surface

ranges from 8.2% to 13.9% with averages of 11.7% (LCL) and 11.4% (CCL), in both cases related to BI 2. Finally, values from bottom intervals range from 0.2% to 3.9%, with mean values of 1.7% (LCL) and 2.9% (CCL), corresponding to BI 1 in both cases. In middle and bottom intervals, BI classification based on a single image would be the same as that obtained from the mean values.

4. Discussion. Linear vs Circumferential Computed Laminography (LCL vs CCL)

The application of Computed Laminography (CL) on cores from modern deep-sea sediments has provided useful images for characterising the trace-fossil assemblage and the intensity of bioturbation at these core sites, without splitting the cores. Additionally, the results obtained from Linear and Circumferential Computed Laminography (LCL and CCL) images are compared, to discuss in which particular situations each technique would be more useful.

4.1. Trace fossil characterization

The obtained results reveal that trace fossil visualization is much better after treating the CL images (Figs. 3, 5). Our analysis of treated images allowed the discernment of a trace-fossil assemblage composed of 13 ichnogenera according to morphological features.

There were no notable differences in trace-fossil identification when comparing assemblages under LCL and CCL methods. All the characterised structures were identified in both LCL and CCL images, but in general they are easier to identify with LCL. Morphological features of some trace fossils used as diagnostic criteria are sometimes distorted when working with CCL images. A clear example can be seen by comparing *Zoophycos* from Linear and Circumferential images (Fig. 7). The images from LCL are equivalent to the exposed surfaces usually analysed when logging cores in the laboratory, making ichnological identification easier. However, there are certain cases in which the use of one or the other kind of image is preferable [to resolve uncertainties in trace fossil identification].

For example, planar trace fossils that cross the entire core can be more easily identified when working with CCL images (Fig. 7A). Such is the case of *Zoophycos*, which can on occasion be confused with some cylindrical meniscated trace fossils (e.g., *Taenidium*) in LCL images in a longitudinal section (Fig. 7B). This uncertainty could also be solved by checking LCL images from different depths, but it is easier and faster in the case of circumferential images, as it can be resolved in a single image.

Yet if identification is based solely on CCL images, some questions will remain unresolved. One example would be the observation of two cross-sections of cylindrical burrows (e.g., *Thalassinoides*) in one image (Fig. 8). In this case, there is no way to tell whether these sections are from the same burrow (Fig. 8A) or different galleries (Fig. 8B).

Accordingly, either of the two CL techniques can be used to characterise trace fossils, but a combination of both is recommended to solve uncertainties in particular cases.

4.2. Intensity of bioturbation

The bioturbated surface was quantified in every LCL and CCL image in order to: 1, analyse differences between images from the same technique; and 2, compare results obtained with different techniques, both in the whole core and in shorter intervals. Considering the illustrated core as a representative example (subsample 15 in BC049; Fig. 6), representative values from the whole section can be obtained either from LCL or CCL, even if the estimation is based on a single image (6.0–8.5%; Table 1). In all cases, the percentage of bioturbated surface corresponds to BI 2. However, differences are higher when working with shorter intervals, being especially notable in the top intervals (standard deviation 3.3%, Table 1). The difference between mean values from LCL and CCL in top intervals is just 1.3%, but this is enough to alter its BI classification. Moreover, the values obtained from single image analysis result in larger differences, the bioturbation intensity varying by up to 10% between some images (i.e., 0.9% vs 10.9%). This would classify some images from the same core as BI 1 (1–4%) and others as 2 (5–30%). The differences are mainly related with longitudinal sections of subhorizontal burrows or the presence of vertical structures that are cut only in a few slices. The situation is similar in middle and deep tier intervals, although differences are lower than the ones registered in the top intervals. These observations reveal that quantification based on just one image is not advisable; rather, it is best to derive the mean value after analysing as many sections as practicable, especially when working with short intervals.

Comparing LCL and CCL, it can be affirmed that mean values obtained from all the slices are very similar when considering the whole section length, but also shorter intervals (Fig. 6, Table 1). Given these differences and taking into account that mean values from CCL are obtained just by analysing two images, and that it is less time-consuming, a quantification based on CCL images is recommended, but avoiding the regions where visibility is limited.

5. Conclusions

The present study confirms the usefulness of Computed

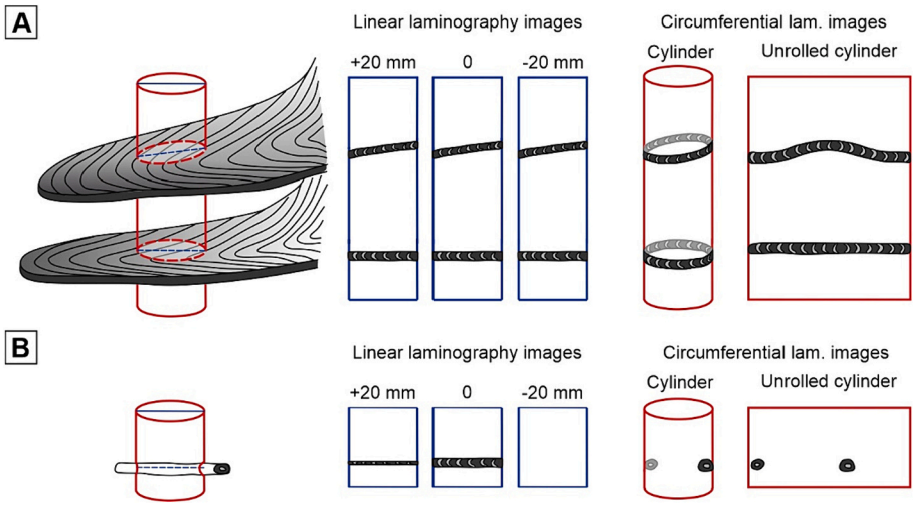

Fig. 7. Schematic diagram of outputs from *Zoophycos* (A) and *Taenidium* (B) in LCL and CCL images.

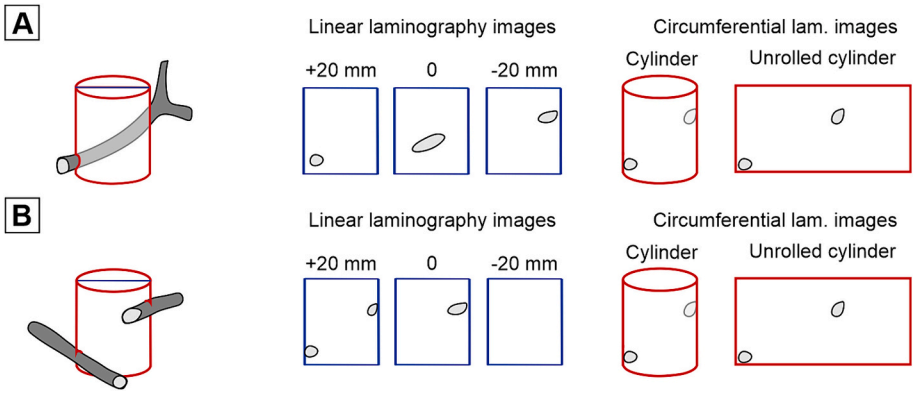

Fig. 8. Schematic diagram of outputs from a controversial situation with one (A) and two (B) cylindrical burrows crossing the study core.

Laminography (CL) for the study of ichnological content of sediment cores, and even some other internal structures, improving the characterization of trace fossils and quantification of the intensity of bioturbation. Additionally, the comparison between Linear Computed Laminography (LCL) and Circumferential Computed Laminography (CCL) reveals that both techniques offer similar results. Still, the integration of both is highly recommended for certain doubtful situations (e.g., *Zoophycos* vs *Taenidium* in some cases).

Regarding the quantification of bioturbation, the use of CCL images is less time-consuming, but it is important to consider excluding the vertical areas where visibility is nil. This aspect need not be considered in quantification from LCL images, but a higher number of images must be analysed to obtain an accurate estimation.

Therefore, the use of CL is highly recommended for the study of internal structures of sediment cores, especially in those cases in which CT data are unavailable or the database size is too large to be processed with the available computational resources.

This study is a first step in the application of Computed Laminography for the analysis of sediment cores, but a promising future is envisaged regarding studies focused on ichnology and other internal structures.

Authorship contribution statement

JD and FJR-T had the original idea for this study. MSJC and OM-S led the data acquisition. JD organised and coordinated the work. JD, FJR-T and OM-S analysed and discussed the results. JD wrote the original draft and all the authors revised and approved the manuscript.

CRediT authorship contribution statement

Javier Dorador: Writing – original draft, Supervision, Methodology, Investigation, Formal analysis, Conceptualization. **Francisco J. Rodríguez-Tovar:** Writing – review & editing, Project administration, Conceptualization. **Miros S.J. Charidemou:** Writing – review & editing, Data curation. **Olmo Miguez-Salas:** Writing – review & editing, Data curation.

Declaration of competing interest

All the authors approve the manuscript and confirm that all the results and interpretations therein are original and have not been previously published. Moreover, we declare there is not any conflict of interest associated with the present contribution.

Data availability

All the processed images and data used in this article are archived in an open repository and freely available for download (https://zenodo.org/records/10404286).

Acknowledgments

This study is supported by Grants TED2021-131697B-C22, and PID2019-104625RB-100 funded by MCIN/AEI/10.13039/501100011033, Grant C-EXP-254-UGR23 funded by Consejería de Universidad, Investigación e Innovación and by ERDF Andalusia Program 2021-2027, and by Research Group RNM-178 funded by Junta de Andalucía. The research by JD was funded through the Ramón y Cajal Fellowship (RYC2021-032385-I) by the Spanish Ministry of Science and Innovation. O M-S is funded by a Humboldt Postdoctoral Fellowship from the Humboldt Foundation, and a Margarita Salas Fellowship from the Ministry of Spain and EU Next Generations projects. We thank the crew and science party of RRS James Cook cruise 231. This work was further supported by the UK Natural Environment Research Council (NERC), through the Climate Linked Atlantic Sector Science project (NE/R015953/1), and it contributes to the Climate Linked Atlantic Sector Science (CLASS) Early Career Researchers project "Bioturbation core analysis of PAP abyssal hill and plains" of O M-S. Funding for open access charge: Universidad de Granada / CBUA. This paper benefited from review by two anonymous reviewers.

References

Aller, J.Y., Aller, R.C., 1986. Evidence for localized enhancement of biological associated with tube and burrow structures in deep-sea sediments at the HEEBLE site, western North Atlantic. Deep-Sea Res. 33, 755–790.

Alonso, B., Ercilla, G., Casas, D., Stow, D.A.V., Rodríguez-Tovar, F.J., Dorador, J., Hernández-Molina, F.J., 2016. Contourite vs gravity-flow deposits of the Pleistocene Faro Drift (Gulf of Cadiz): sedimentological and mineralogical approaches. Mar. Geol. 377, 77–94.

Andrews, J.T., Smith, L.M., Preston, R., Cooper, T., Jennings, A.E., 1997. Spatial and temporal patterns of iceberg rafting (IRD) along the East Greenland margin, ca. 68°N, over the last 14 cal.Ka. J. Quat. Sci. 12, 1–13.

Bertling, M., Buatois, L.A., Knaust, D., Laing, B., Mángano, M.G., Meyer, N., Mikuláš, R., Minter, N.J., Neumann, C., Rindsberg, A.K., Uchman, A., 2022. Names for trace fossils 2.0: theory and practice in ichnotaxonomy. Lethaia 55 (3), 1–19.

Boespflug, X., Long, B.F.N., Occhietti, S., 1995. CAT-scan in marine stratigraphy: a quantitative approach. Mar. Geol. 122, 281–301.

Bromley, R.G., 1996. Trace Fossils: Biology, Taphonomy and Applications. Chapman & Hall, London, p. 361.

Bull, D.J., Helfen, L., Sinclair, I., Spearing, S.M., Baumbach, T., 2013. A comparison of multi-scale 3D X-ray tomographic inspection techniques for assessing carbon fibre composite impact damage. Compos. Sci. Technol. 75, 55–61.

Cnudde, V., Boone, M.N., 2013. High-resolution X-ray computed tomography in geosciences: a review of the current technology and applications. Earth Sci. Rev. 123, 1–17.

Dashtgard, S.E., Snedden, J.W., MacEachern, J.A., 2015. Unbioturbated sediments on a muddy shelf: Hypoxia or simply reduced oxygen saturation? Palaeogeogr. Palaeoclimatol. Palaeoecol. 425, 128–138.

Dorador, J., Rodríguez-Tovar, F.J., 2016. Stratigraphic variation in ichnofabrics at the "Shackleton Site" (IODP Site U1385) on the Iberian margin: paleoenvironmental implications. Mar. Geol. 377, 118–126.

Dorador, J., Rodríguez-Tovar, F.J., 2018. High-resolution image treatment in ichnological core analysis: initial steps, advances and prospects. Earth Sci. Rev. 177, 226–237.
Dorador, J., Rodríguez-Tovar, F.J., 2020. CroSSED sequence, a new tool for 3D processing in geosciences using the free software 3DSlicer. Sci. Data 7, 270.
Dorador, J., Wetzel, A., Rodríguez-Tovar, F.J., 2016. *Zoophycos* in deep-sea sediments indicates high and seasonal primary productivity: Ichnology as a proxy in palaeoceanography during glacial-interglacial variations. Terra Nova 28, 323–328.
Dorador, J., Rodríguez-Tovar, F.J., Titschack, J., 2020. Exploring computed tomography in ichnological analysis of cores from modern marine sediments. Sci. Rep. 10, 201.
Dowdeswell, J.A., Whittington, R.J., Jennings, A.E., Andrews, J.T., Mackensen, A., Marienfeld, P., 2000. Sedimentology 47, 557–576.
Durden, J.M., Bett, B.J., Jones, D.O.B., Huvenne, V.A.I., Ruhl, H.A., 2015. Abyssal hills – hidden source of increased habitat heterogeneity, benthic megafaunal biomass and diversity in the deep sea. Prog. Oceanogr. 137, 209–218. https://doi.org/10.1016/j.pocean.2015.06.006.
Durden, J.M., Bett, B.J., Ruhl, H.A., 2020. Subtle variation in abyssal terrain induces significant change in benthic megafaunal abundance, diversity, and community structure. Prog. Oceanogr. 186, 102395 https://doi.org/10.1016/j.pocean.2020.102395.
Ellis, B.R., Fitts, J.P., Bromhal, G.S., McIntyre, D.L., Tappero, R., Peters, C.A., 2013. Dissolution-driven permeability reduction of a fractured carbonate caprock. Environ. Eng. Sci. 30, 187–193.
Eltom, H.A., Nanda Syahputra, M.R., El-Husseiny, A., La Croix, A.D., 2023. Spatial complexity of burrow attributes and their impact on porosity and permeability distributions in bioturbated reservoirs. Sediment. Geol. 450, 106395.
Fisher, S.L., Holmes, D.J., Jørgensen, J.S., Gajjar, P., Behnsen, J., Lionheart, W.R.B., Withers, P.J., 2019. Laminography in the lab: imaging planar objects using a conventional x-ray CT scanner. Meas. Sci. Technol. 30, 035401.
Gérard, J., Bromley, R.G., 2008. Ichnofabrics in Clastic Sediments: Applications to Sedimentological Core Studies. Jean R. F. Gerard.
Gondrom, S., Zhou, J., Maisl, M., Reiter, H., Kröning, M., Arnold, W., 1999. X-ray computed laminography: an approach of computed tomography for applications with limited access. Nucl. Eng. Des. 190, 141–147.
González-Lanchas, A., Dorador, J., Rodríguez-Tovar, F.J., Sierro, F.J., Flores, J.A., 2022. Trace fossil characterization during termination V and MIS 11 at the western Mediterranean: connection between surface conditions and deep environment. Mar. Geol. 446, 106774.
Gougeon, R.C., Mángano, M.G., Buatois, L.A., Narbonne, G.M., Laing, B.A., 2018. Early Cambrian origin of the shelf sediment mixed layer. Nat. Commun. 9, 1909.
Hartman, S., 2022. Time-Series Studies at the Porcupine Abyssal Plain Sustained Observatory. National Oceanography Centre Research Expedition Report, Southampton, National Oceanography Centre, p. 201.
Helfen, L., 2005. High-resolution three-dimensional imaging of flat objects by synchrotron-radiation computed laminography. Appl. Phys. Lett. 86, 071915.
Hodell, D.A., Nicholl, J.A., Bontognali, T.R.R., Danino, S., Dorador, J., Dowdeswell, J.A., Einsle, J., Kuhlmann, H., Martrat, B., Mleneck-Vautravers, M.J., Rodríguez-Tovar, F. J., Röhl, U., 2017. Anatomy of Heinrich Layer 1 and its role in the last deglaciation. Paleoceanogr. Paleoclimatol. 32, 284–303.
Houssaye, A., Xu, F., Helfen, L., De Buffrénil, V., Baumbach, T., Tafforeau, P., 2011. Three-dimensional pelvis and limb anatomy of the Cenomanian hind-limbed snake *Eupodophis descouensi* (Squamata, Ophidia) revealed by synchrotron-radiation computed laminography. J. Verteb. Paleontol. 3, 12-7.
Knaust, D., 2012. Methodology and techniques. In: Knaust, D., Bromley, R.G. (Eds.), Trace Fossils as Indicators of Sedimentary Environments. Developments of Sedimentology 64. Elsevier, pp. 245–271.
Knaust, D., 2017. Atlas of Trace Fossils in Well Core: Appearance. Springer, Taxonomy and Interpretation.
Konno, Y., Jin, Y., Yoneda, J., Uchiumi, T., Shinjou, K., Nagao, J., 2016. Hydraulic fracturing in methane-hydrate-bearing sand. RSC Adv. 6, 73148–73155.
Legrand, S., Vanmeert, F., Van der Snickt, G., Alfeld, M., De Nolf, W., Dik, J., Janssens, K., 2014. Examination of historical paintings by state-of-the-art hyperspectral imaging methods: from scanning infra-red spectroscopy to computed X-ray laminography. Heritage Sci. 2, 13.
Löwemark, L., 2007. Importance and usefulness of trace fossils and bioturbation in paleoceanography. In: Miller III, W. (Ed.), Trace Fossils, Concepts, Problems, Prospects. Elsevier, pp. 127–413.
McDonald, N., Bradwell, T., Callard, S.L., Toney, J.L., Shreeve, B., Shreeve, J., 2022. Automated characterisation of glaciomarine sediments using X-ray computed laminography. Quatern. Sci. Adv. 5, 100046.
Moore, T.D., Vanderstraeten, D., Forssell, P.M., 2002. Three-dimensional x-ray laminography as a tool for detection and characterization of BGA package defects. IEEE Trans. Comp. Packag. Technol. 25, 224–229.
Morgeneyer, T.F., Helfen, L., Sinclair, I., Proudhon, H., Xu, F., Baumbach, T., 2011. Ductile crack initiation and propagation assessed via in situ synchrotron radiation-computed laminography. Scripta Materialia 65, 1010–1013.
O'Brien, N.S., Boardman, R.P., Sinclair, I., Blumensath, T., 2016. Recent advances in X-ray Cone-beam Computed Laminography. J. Xray Sci. Technol. 24, 691–707.
Orsi, T.H., Edwards, C.M., Anderson, A.L., 1994. X-ray computed tomography: a nondestructive method for quantitative analysis of sediment cores. J. Sediment. Res. A: Sediment. Petrol. Proces. A64, 690–693.
Reineck, H.-E., 1963. Sedimentgefüge im Bereich der südliche Nordsee. Abh. Senckenb. Naturforsch. Ges. 505, 1–138.
Rodríguez-Tovar, F.J., Dorador, J., Martín-García, G.M., Sierro, F.J., Flores, J.A., Hodell, D.A., 2015. Response of macrobenthic and foraminifer communities to changes in deep-sea environmental conditions from Marine Isotope Stage (MIS) 12 to 11 at the "Shackleton Site". Glob. Planet. Chang. 133, 176–187.
Taylor, A.M., Goldring, R., 1993. Description and analysis of bioturbation and ichnofabric. J. Geol. Soc. Lond. 150, 141–148.
Teal, L.R., Bulling, M.T., Parker, E.R., Solan, M., 2008. Global patterns of bioturbation intensity and mixed depth of marine soft sediments. Aquat. Biol. 2, 207–218.
Valencia, F.L., Mángano, M.G., Buatois, L.A, Laya, J.C., 2022. Animal–substrate interactions preserved in ancient lagoonal chalk. Sci. Rep. 12, 14383.
Verboven, P., Herremans, E., Helfen, L., Ho, Q.T., Abera, M., Baumbach, T., Wevers, M., Nicolaï, B.M., 2015. Synchrotron X-ray computed laminography of the three-dimensional anatomy of tomato leaves. Plant J. 81, 169–182.
Wang, Y., Wang, X., Hu, B., Uchman, A., 2019. Burrows of the polychaete *Perinereis aibuhiutensis* on a tidal flat of Yellow River Delta in China: Implications for the ichnofossils *Polykladichnus* and *Archaeonassa*. Palaios 34, 271–279.
Wetzel, A., 2010. Deep-sea ichnology: Observations in modern sediments to interpret fossil counterparts. Acta Geol. Pol. 60, 125–138.
Xu, F., Helfen, L., Baumbach, T., Suhonen, H., 2012. Comparison of image quality in computed laminography and tomography. Opt. Express 20, 795–806.
Zuber, M., Laaß, M., Hamann, E., Kretschmer, S., Hauschke, N., van de Kamp, T., Baumbach, T., Koenig, T., 2017. Augmented laminography, a correlative 3D imaging method for revealing the inner structure of compressed fossils. Sci. Rep. 7, 41413.